
Learned Step Size Quantization

Steven K Esser¹ Jeffrey L. McKinstry¹ Deepika Bablani¹ Rathinakumar Appuswamy¹
Dharmendra S. Modha¹

Abstract

We present here Learned Step Size Quantization, a method for training deep networks such that they can run at inference time using low precision integer matrix multipliers, which offer power and space advantages over high precision alternatives. The essence of our approach is to learn the step size parameter of a uniform quantizer by backpropagation of the training loss, applying a scaling factor to its learning rate, and computing its associated loss gradient by ignoring the discontinuity present in the quantizer. This quantization approach can be applied to activations or weights, using different levels of precision as needed for a given system, and requiring only a simple modification of existing training code. As demonstrated on the ImageNet dataset, our approach achieves better accuracy than all previous published methods for creating quantized networks on several ResNet network architectures at 2-, 3- and 4-bits of precision.

1. Introduction

Deep networks are emerging as components of a number of revolutionary technologies, including image recognition (Krizhevsky et al., 2012), speech recognition (Hinton et al., 2012), and driving assistance (Xu et al., 2017). Unlocking the full promise of such applications requires a system perspective where task performance, throughput, energy-efficiency, and compactness are all critical considerations to be optimized through co-design of algorithms and deployment hardware. Current research seeks to create deep networks that maintain high accuracy while reducing the precision needed to represent their activations and weights, thereby reducing the computation and memory required for their implementation. The advantages of using such low precision algorithms to create networks for low precision hardware has been demonstrated in several deployed

systems (Esser et al., 2016; Jouppi et al., 2017; Qiu et al., 2016). Here we demonstrate a new method for training quantized networks that achieves significantly better performance than prior quantization approaches on the ImageNet dataset across several network architectures.

Our primary contribution is *Learned Step Size Quantization* (LSQ), a method for training low precision networks that uses the training loss gradient to learn the step size parameter of a uniform quantizer associated with each layer of weights and activations. While there are many methods of quantizing data, most approaches apply a sequence of operations that first scale the data, then round and clip the data to a set of integer values whose range is determined by the number of quantization bits, and then finally rescale the data back to its original range. Strictly speaking, this process is not differentiable due to the use of the round operator, but approximations can be employed to allow for backpropagation. Prior approaches that use backpropagation to learn parameters controlling quantization (Choi et al., 2018b;a; Jung et al., 2018) create a gradient approximation by beginning with the forward function for the quantizer, removing the round function from this equation, then differentiating the remaining operations. In contrast, our approach simply differentiates each operation of the quantizer forward function, passing the gradient through the round function, but allowing the round function to impact down stream operations in the quantizer for the purpose of computing their gradient. As we discuss below, these two methods lead to different gradients to parameters controlling the quantization itself, with our approach producing a gradient with finer responsiveness across the domain of the quantizer.

Many approaches have been explored for training networks for low precision inference. These have included quantizers where the mapping from inputs to discrete values is i) fixed based on user settings, ii) tuned using statistics from the data, iii) tuned by solving a quantizer error minimization problem during training, or iv) learned using backpropagation to train parameters controlling the quantization process. Uniform quantization is commonly employed, but a few approaches employ asymmetric (different quantization for positive and negative values) or nonuniform mappings, which introduce additional complexity to the quantization process by allowing variable bin sizes. Table 1 summarizes this prior work.

¹IBM Research. Correspondence to: Steven K Esser <ssesser@us.ibm.com>.

Table 1. Quantization approaches, specifying how a mapping is chosen from inputs to quantized values, and how the quantized values themselves are distributed. QE: Quantization Error, Backprop: Backpropagation.

METHOD	QUANTIZER TUNING	QUANTIZER DISTRIBUTION	REFERENCE
BNN	FIXED	UNIFORM	(HUBARA ET AL., 2016)
EEDN	FIXED	UNIFORM	(ESSER ET AL., 2016)
FAQ	FIXED	UNIFORM	(MCKINSTRY ET AL., 2018)
TWN	DATA STATISTICS	UNIFORM	(LI & LIU, 2016)
DoReFA	DATA STATISTICS	UNIFORM	(ZHOU ET AL., 2016)
XNOR	DATA STATISTICS	UNIFORM	(RASTEGARI ET AL., 2016)
HWGQ	DATA STATISTICS	UNIFORM	(CAI ET AL., 2017)
REGULARIZATION	QE MINIMIZATION	UNIFORM	(CHOI ET AL., 2018C)
LQ-NETS	QE MINIMIZATION	NONUNIFORM	(ZHANG ET AL., 2018)
QIL	BACKPROP	UNIFORM	(JUNG ET AL., 2018)
NICE	BACKPROP	UNIFORM	(BASKIN ET AL., 2018)
DISTILLATION	BACKPROP	NONUNIFORM	(POLINO ET AL., 2018)
LSQ (OURS)	BACKPROP	UNIFORM	
TTQ	BACKPROP + DATA STATISTICS	UNIFORM, ASYMMETRIC	(ZHU ET AL., 2016)
APPRENTICE	BACKPROP + DATA STATISTICS	UNIFORM, ASYMMETRIC	(MISHRA & MARR, 2017)
PACT	BACKPROP + DATA STATISTICS	UNIFORM	(CHOI ET AL., 2018B)
PACT-SAWB	BACKPROP + DATA STATISTICS	UNIFORM	(CHOI ET AL., 2018A)

Our approach falls in the school of directly learning quantization parameters through backpropagation, which has the appealing feature that it seeks a quantization that directly improves the metric of interest, the training loss. In comparison, fixed mapping schemes based on user settings, while attractive for their simplicity, place no guarantees on optimizing network performance, and quantization error minimization schemes might perfectly minimize quantization error and yet still be non optimal if a different quantization mapping actually minimizes task error. The primary differences of our approach from previous work using backpropagation to learn the quantization mapping are the use of a different approximation to the quantizer gradient, described in detail in Section 2.1, and the application of a scaling factor to the learning rate of the parameters controlling quantization.

2. Methods

Our objective is to train a deep network such that, at inference time, the matrix multiplication operations used in its convolution and fully connected layers can be implemented using low precision integer operations. Our specific approach is to employ a uniform quantizer of the form:

$$\bar{v} = \lfloor \text{clip}(v/s, L) \rfloor, \quad (1)$$

$$\hat{v} = \bar{v} \times s, \quad (2)$$

where v is the data to quantize, \bar{v} is a quantized, scaled integer representation of the data, \hat{v} is the quantized output at the same scale as v , s is a step size parameter, $\lfloor z \rfloor$ rounds z

to the nearest integer, and $\text{clip}(z, r)$ is a signed clip function that returns z with values below $-r$ set to $-r$ and values above r set to r . For unsigned data, L is the number of positive non-zero quantization levels, and for signed data L is the number of positive and the number of negative non-zero quantization levels. Thus for an encoding using b bits, $L = 2^b - 1$ for unsigned data, and $L = 2^{b-1} - 1$ for signed data (which uses one state less than available given b bits so as to preserve symmetry about zero).

For inference, we envision computing equation 1 for weights (w) offline, for activations (x) online, and using the resulting \bar{w} and \bar{x} values as input to low precision integer matrix multiplication units underlying convolution or fully connected layers. The output of such layers can then be rescaled by the step size for weights (s_w) and activations (s_x) using a relatively low cost high precision scalar-tensor multiplication, a step that can potentially be merged with other operations such as the affine transform associated with batch normalization. A simple visualization of this computational flow is provided in Figure 1.

To train our network, we follow the now widely adopted practice for training quantized networks of maintaining and updating full precision weights, but using quantized weights and activations for the forward pass. For simplicity during training, we use \hat{v} as input to matrix multiplication layers, which is algebraically equivalent to our proposed inference operations described in the preceding paragraph. For the gradient through the quantization functions to activations, we use a straight through estimator for the round function gradient (Bengio et al., 2013), and set the gradient of clipped

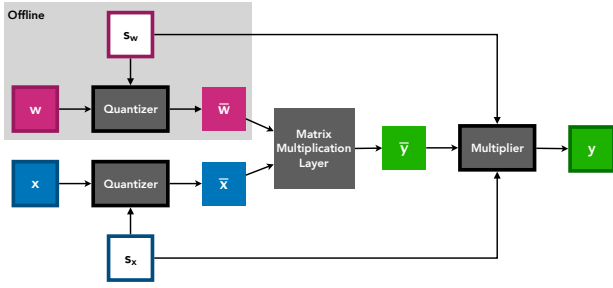


Figure 1. Data flow diagram for computations involved for a single low precision convolution or fully connected layer, as envisioned here. Boxes without borders denote low precision integer data or operations.

values to zero:

$$\frac{\partial \hat{x}}{\partial x} = \begin{cases} 1 & \text{if } |x| < L, \\ 0 & \text{otherwise.} \end{cases} \quad (3)$$

For the gradient through the quantizer to weights, we also use a straight through estimator for the round function but pass the gradient completely through the clip function as this avoids weights becoming permanently stuck in the clipped range:

$$\frac{\partial \hat{w}}{\partial w} = 1. \quad (4)$$

2.1. Learned Step Size Quantization

The step size parameter determines the specific mapping of high precision to quantized values, which can have a large impact on network performance (in a worst case, an arbitrarily large step size would map all values to zero). Since our objective during learning is to minimize training loss, we choose to learn step size in a way that also seeks to minimize this loss, specifically by treating s as a parameter to be learned using standard backpropagation. To backpropagate to the step size parameter requires an approximation of the gradient of the quantizer output with respect to step size, $\partial \hat{v} / \partial s$, which is otherwise undefined due to the discontinuous nature of the quantizer.

Here, we propose to approximate $\partial \hat{v} / \partial s$ by using a straight through estimator for the round function in the quantizer, as used in computing $\partial \hat{v} / \partial v$ above, and applying standard differentiation for the remaining operations in the quantizer, including setting the gradient of clipped values to zero. It should be noted that we do not remove the round function itself where it would naturally appear in the gradient equation (specifically, the component of $\partial \hat{v} / \partial s$ derived from the appearance of s in equation 2 is dependent on this round

function):

$$\frac{\partial \hat{v}}{\partial s} = \begin{cases} -v/s + \lfloor v/s \rfloor & \text{if } |v/s| < L \\ \hat{v}/s & \text{otherwise.} \end{cases} \quad (5)$$

This gradient is visualized in Figure 2.

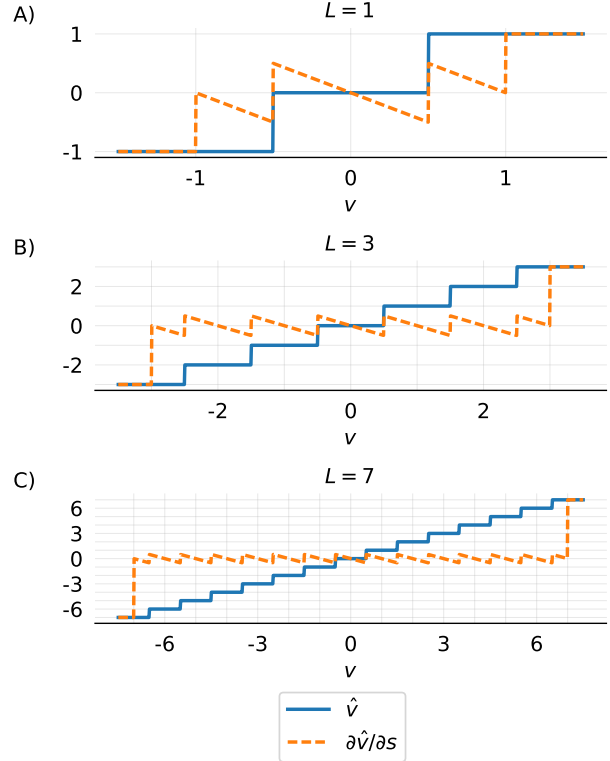


Figure 2. Quantizer output and our approximated gradient with respect to the step size parameter where $s = 1$ and A) $L = 1$, corresponding to use of 2-bit weights, B) $L = 3$, corresponding to 3-bit weights and the positive portion corresponding to 2-bit activations, and C) $L = 7$, corresponding to 4-bit weights and the positive portion corresponding to 3-bit activations.

To provide a deeper understanding of this gradient, it can be noted that s appears twice in the quantizer. In equation 1, s appears as a divisor inside the round function, where it determines which integer valued quantization bin (\bar{v}) each real valued input is assigned. The gradient with respect to s at this location provides the first term in equation 5 when $|v/s| < L$, and does not have an impact when $|v/s| \geq L$ as we do not pass the gradient to this appearance of s for values clipped in the forward pass. The negative sign on this term reflects the fact that as s in equation 1 increases, there is a chance that \bar{v} will drop to a lower magnitude bin.

In equation 2, s appears as a multiplier outside of the round function, where it determines the real value (\hat{v}) to which each integer value maps. The gradient with respect to this

appearance of s provides the second term in equation 5 when $|v/s| < L$ and the entire gradient when $|v/s| \geq L$. The associated positive sign on these terms reflects the fact that as s in equation 2 increases, \hat{v} will increase proportional to $\text{clip}(\lfloor v/s \rfloor, L)$.

Prior approaches using backpropagation to learn quantization controlling parameters (Choi et al., 2018b;a; Jung et al., 2018) completely remove the round operation when differentiating the forward pass, equivalent in our derivation to removing the round function in equation 5, so that where $|v/s| < L$ the two terms cancel such that $\partial\hat{v}/\partial s = 0$. This provides a coarser approximation of this gradient, one drawback of which is that $\partial\hat{v}/\partial s = 0$ if $\hat{v} = 0$. However, consider that if v is just less than $0.5s$, a very small decrease in s will cause the corresponding \hat{v} to change from 0 to s , suggesting that the gradient in this region should be non zero.

For this work, each layer of weights has a distinct s and each layer of activations has a distinct s , thus the number of step size parameters in a given network is equal to the number of quantized weight layers plus the number of quantized activation layers. Step size is initialized for activations to 1, and for weight layers to the average absolute value of the weights. We implemented and tested LSQ in PyTorch.

2.2. Step Size Learning Rate Scale

We note that for a given layer, if the updates to s as a result of learning are large relative to changes to v_i , then changes to \hat{v}_i could become highly correlated, driven by the single source s . This would likely impact the quality of learning, as it is of course desirable that each \hat{v}_i in a given population changes independently to promote diverse responses to different inputs.

The magnitude of a parameter update for a given mini-batch in stochastic gradient descent is proportional to its gradient with respect to training loss, E . For s , this gradient is:

$$\frac{\partial E}{\partial s} = \sum_i \frac{\partial E}{\partial \hat{v}_i} \frac{\partial \hat{v}_i}{\partial s}, \quad (6)$$

where i is over all elements in the corresponding layer. This summation over the population could result in $\partial E/\partial s$ much larger than a typical $\partial E/\partial v_i$, particularly if values of $\partial E/\partial \hat{v}_i$ are highly correlated, leading to changes in s with a magnitude greatly differing from changes to v_i . To prevent this imbalance from leading to instability in learning, we introduce a *step size learning rate scale* hyperparameter that is simply a multiplier on the learning rate used for s . For simplicity, we use a single such hyperparameter for all weight layers, and a single such hyperparameter for all activation layers. We found that properly setting the learning rate scale was critical to good performance and chose values via experiment on a 2-bit ResNet-18 network (see Section

3.1).

2.3. Fine Tuning

All of the quantized networks in this paper use fine tuning, that is they are initialized using weights from a trained full precision network with equivalent architecture before training in the quantized space. This approach has been explored in a number of works as means to improve training of quantized networks (Sung et al., 2015; Zhou et al., 2016; Mishra & Marr, 2017; McKinstry et al., 2018).

2.4. Dataset

All experiments in this paper were conducted on the ImageNet dataset (Russakovsky et al., 2015). For the purpose of performing hyperparameter exploration without knowledge of the final validation set, we split the ImageNet training dataset into two subsets by moving 50 training images from each class to a new data set we call *train-v*, used for validation during hyperparameter sweeps, and using the remaining training images for another dataset we call *train-t*, used for the corresponding training. All results in this paper use the standard ImageNet training and validation sets, except where it is explicitly noted that they use *train-v* and *train-t*.

2.5. Training Procedure

All networks were trained using stochastic gradient descent optimization with a momentum of 0.9, using a softmax cross entropy loss function and cosine learning rate decay (Loshchilov & Hutter, 2016) (without restarts). Full precision controls were trained with weight decay of 0.0001, with ResNet18 and ResNet34 using a learning rate of 0.1 and batch size of 256, and ResNet50 using a learning rate of 0.05 and batch size of 128. Quantized networks were trained with weight decay of 0.00005 for ResNet18, and weight decay of 0.0001 for the larger ResNet34 and ResNet50 as suggested in (McKinstry et al., 2018), all with an initial learning rates 10 times lower the full precision networks and the same batch size as the full precision controls. Except where noted, all networks were trained for 90 epochs. Images were resized to 256×256 , then a 224×224 crop was selected for training, with horizontal mirroring applied randomly with 0.5 probability. At test time, a 224×224 centered crop was chosen.

Experiments were run using the pre-activation version of ResNet (He et al., 2016). We use high precision input activations and weights for the first and last layers, as this standard practice for quantized neural networks has been demonstrated to make a large impact on performance.

3. Results

In the sections below, we first perform hyperparameter sweeps to determine the value of step size learning rate scale to use. Following this we look at the distribution of quantized data, examine quantization error, then compare LSQ to existing quantization methods across several network architectures.

3.1. Step Size Learning Rate Scale Hyperparameter Sweep

To select the weight step size learning rate scale, we trained 6 ResNet-18 networks with 2-bit activations and full precision weights for 9 epochs, setting the learning rate scale to a different member of the set $\{10^0, 10^{-1}, \dots, 10^{-5}\}$ for each run, and using the ImageNet train-v and train-t subsets. We performed a similar sweep for the activation step size learning rate scale with 2-bit weights and full precision activations.

For activations, we found best performance with a step size learning rate scale of 10^{-1} , with performance falling off steadily as this value was reduced (Figure 3A). For weights, we found a broad plateau in the hyperparameter space that provided good performance with a step size learn rate scale between 10^{-2} and 10^{-4} , with best performance at 10^{-4} (Figure 3B). Based on this, for all further training we used an activation step size learning rate scale of 10^{-1} and a weight step size learning rate scale of 10^{-4} . In all remaining sections we used the real ImageNet train and validation sets.

3.2. Distribution of Quantized Data

We examined the distribution of quantized data in a trained ResNet-18 network with 2-bit activations and weights by computing a histogram of \bar{v} for each layer for all data in the test set (Figure 4). We noted that activations were biased towards the zero bin with 64.7% of activations in the zero bin, a result not particularly surprising given the use of ReLU neurons in the network. Weights showed a slight preference for the zero bin, with 44.3% of weights quantized to zero.

3.3. Quantization Error

LSQ seeks a quantization that explicitly minimizes training loss and not quantization error (the distance between \hat{v} and v on some metric). We next sought to understand whether LSQ learns a final step size that also implicitly minimizes quantization error. For this purpose, for a given layer we define the final step size learned by LSQ as \hat{s} and let S be the set of discrete values $\{0.01\hat{s}, 0.02\hat{s}, \dots, 20.00\hat{s}\}$. For each layer, on a single batch of test data we computed which value of $s \in S$ minimizes mean absolute error, $E[|(\hat{v}(s) - v)|]$, mean square error, $E[(\hat{v}(s) - v)^2]$, and Kullback-Leibler

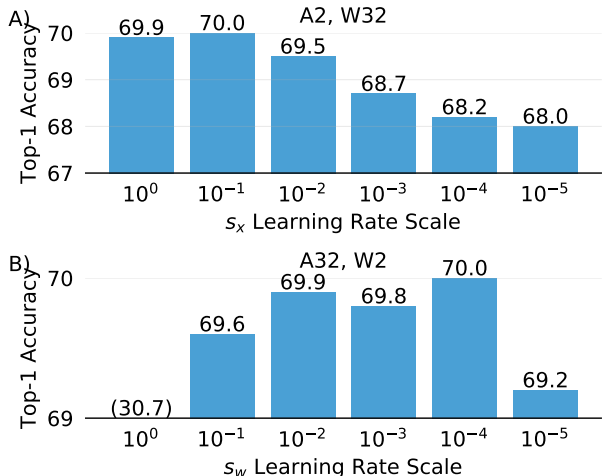


Figure 3. Hyperparameter sweep of step size learning rate scale using 9 epoch training runs on ResNet-18. A) Sweep for activation step size, using 2-bit activations and full precision weights. B) Sweep for weight step size, using 2-bit weights and full precision activations. The corresponding numeric top-1 accuracy is given above each bar, with a number in parentheses indicating the value is too low for the bar to appear within the range shown.

divergence, $\int p(v) \log p(v) - \int p(v) \log q(\hat{v}(s))$ where p and q are probability distributions. For purposes of relative comparison, we ignore the first term of Kullback-Leibler divergence, as it does not depend on \hat{v} , and approximate the second term as $-E[\log(q(\hat{v}(s)))]$, where the expectation is over the sample distribution.

Per layer results of the above comparison are shown in Figure 5. To provide a condensed measurement of quantization error, we computed the absolute difference between \hat{s} and the value of s that minimizes each of the above metrics, and averaged this across weight layers and across activation layers (a difference of 0 would indicate the learned value of step size also minimizes the corresponding quantization error metric). For activations, this difference was 0.46 for mean absolute error, 0.83 for mean square error, and 0.60 for Kullback-Leibler divergence, while for weights, this difference was 0.90 for mean absolute error, 3.53 for mean square error, and 0.10 for Kullback-Leibler divergence.

3.4. Comparison with Other Approaches

We used LSQ to train several ResNet variants where activations and weights both use 2, 3 or 4 bits of precision, and compared our results to published results of other approaches for training quantized networks. To facilitate comparison, we did not consider networks that used full precision for any layer other than the first and last. We trained full precision (baseline) versions of the networks we considered

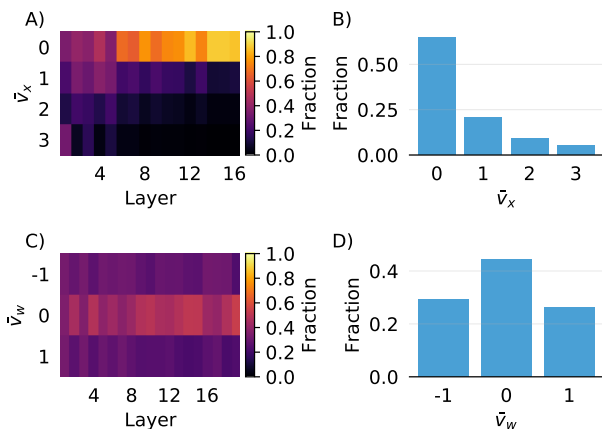


Figure 4. For a trained 2-bit ResNet-18, distribution of quantized integer activation values (\tilde{v}_x) by layer (A) and averaged for all layers (B), and distribution of quantized integer weight values (\tilde{v}_w) by layer (C) and averaged for all layers (D).

and found scores slightly higher than previously reported, which we attribute to our use of cosine learning rate decay (Loshchilov & Hutter, 2016).

On ResNet-18 (Table 2), ResNet-34 (Table 3), and ResNet-50 (Table 4), we found that LSQ achieved higher accuracy than all prior quantization approaches at the precision we examined. Accuracy improved with higher precision, and at 4-bit exceeded baseline full precision accuracy on ResNet-18 (+0.4 top-1) and on ResNet-34 (+0.3 top-1) and nearly matched full precision accuracy on ResNet-50 (−0.2 top-1).

4. Conclusions

The results here demonstrate that LSQ exceeds performance of all prior approaches for creating quantized networks across several architectures for classifying the ImageNet dataset. Interestingly, LSQ does not appear to minimize quantization error, whether measured using mean square error, mean absolute error, or Kullback-Leibler divergence. The approach itself is simple, requiring a single additional parameter per weight or activation layer.

Looking to future work, it is likely possible to constrain the step size parameter to powers of 2 without a large degradation in performance. Such an approach would further simplify the hardware necessary for quantization by replacing the multiplications with bit shift operations. Though it remains to be demonstrated, it is possible that the relative insensitivity of LSQ to the specific step size learning rate scale might also mean that it is relatively tolerant to a range of step sizes, and thus a power of 2 constraint would have relatively little impact on performance.

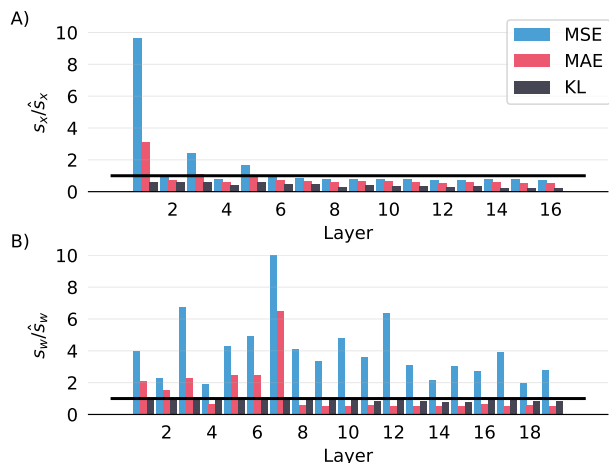


Figure 5. Mean square error (MSE), mean absolute error (MAE) and Kullback-Leibler divergence (KL), between \hat{v} and v for each layer across a range of s for activations (A) and weights (B). To facilitate comparison between layers, s is normalized by the actual step size learned by LSQ (\hat{s}). Horizontal bar indicates where $s = \hat{s}$.

This work is a continuation of a trend towards steadily reducing the number of bits of precision necessary to achieve good performance across a range of network architectures on ImageNet. It is noteworthy that this trend towards higher performance at lower precision strengthens the analogy between artificial neural networks and biological neural networks, which themselves employ synapses represented by perhaps a few bits of information (Bartol Jr et al., 2015) and single bit spikes that may be employed in small spatial and/or temporal ensembles to provide low bit width data representation. Of course, it is yet unclear exactly how far this analogy can be taken. These recent results in the low precision space suggest that compute resources used for performing classification with neural networks require dramatically fewer bits of precision than commonly believed even a few years ago, meaning that custom hardware able to operate at these reduced precision levels could gain considerably from the resulting energy-efficiency and compactness, without sacrificing task performance.

Table 2. Comparison of low precision ResNet-18 networks on ImageNet. An asterisk indicates results are reported in (Choi et al., 2018b), but not in the original paper. Under precision, "nu" indicates non uniform quantization.

METHOD	PRECISION (A,W)	ACCURACY	
		TOP-1	TOP-5
BASELINE (OURS)	32, 32	70.5	89.6
LSQ (OURS)	4, 4	70.9	89.9
QIL	4, 4	70.1	
FAQ	4, 4	69.8	89.1
LQ-NETS	4, 4 (NU)	69.3	88.8
PACT	4, 4	69.2	89.0
NICE	4, 4	69.8	89.2
DoREFA*	4, 4	67.5	87.6
REGULARIZATION	2, 2	67.3	87.9
LSQ (OURS)	3, 3	70.0	89.4
QIL	3, 3	69.2	
LQ-NETS	3, 3 (NU)	68.2	87.9
PACT	3, 3	68.1	88.2
NICE	3, 3	67.7	88.2
DoREFA*	3, 3	67.5	87.6
LSQ (OURS)	2, 2	67.0	87.3
QIL	2, 2	65.7	
LQ-NETS	2, 2 (NU)	64.9	85.9
PACT	2, 2	64.4	85.6
DoREFA*	2, 2	62.6	84.4
REGULARIZATION	2, 2	61.7	84.4

Table 3. Comparison of low precision ResNet-34 networks on ImageNet. An asterisk indicates results are reported in (Choi et al., 2018b), but not in the original paper. Under precision, "nu" indicates non uniform quantization.

METHOD	PRECISION (A,W)	ACCURACY	
		TOP-1	TOP-5
BASELINE (OURS)	32, 32	74.1	91.8
LSQ (OURS)	4, 4	74.4	91.8
QIL	4, 4	73.7	
NICE	4, 4	73.5	91.4
FAQ	4, 4	73.3	91.3
DoREFA*	4, 4	69.9	89.2
LSQ (OURS)	3, 3	73.8	91.4
QIL	3, 3	73.1	
LQ-NETS	3, 3 (NU)	71.9	90.2
NICE	3, 3	71.7	90.8
DoREFA*	3, 3	69.9	89.2
LSQ (OURS)	2, 2	71.1	90.0
QIL	2, 2	70.6	
LQ-NETS	2, 2 (NU)	69.8	89.1
DoREFA*	2, 2	67.1	87.3

Table 4. Comparison of low precision ResNet-50 networks on ImageNet. An asterisk indicates results are reported in (Choi et al., 2018b), but not in the original paper. Under precision, "nu" indicates non uniform quantization.

METHOD	PRECISION (A,W)	ACCURACY	
		TOP-1	TOP-5
BASELINE (OURS)	32, 32	76.9	93.4
LSQ (OURS)	4, 4	76.7	93.3
NICE	4, 4	76.5	93.3
PACT	4, 4	76.5	92.6
FAQ	4, 4	76.3	92.9
LQ-NETS	4, 4 (NU)	75.1	92.4
DoREFA*	4, 4	71.4	89.8
LSQ (OURS)	3, 3	76.1	92.9
PACT	3, 3	75.3	92.6
NICE	3, 3	75.1	92.6
LQ-NETS	3, 3 (NU)	75.1	92.4
DoREFA*	3, 3	69.9	89.2
LSQ (OURS)	2, 2	73.2	91.3
PACT	2, 2	72.2	90.5
LQ-NETS	2, 2 (NU)	71.5	90.3
DoREFA*	2, 2	67.1	87.3

References

- Bartol Jr, T. M., Bromer, C., Kinney, J., Chirillo, M. A., Bourne, J. N., Harris, K. M., and Sejnowski, T. J. Nanoconnectomic upper bound on the variability of synaptic plasticity. *Elife*, 4:e10778, 2015.
- Baskin, C., Liss, N., Chai, Y., Zheltonozhskii, E., Schwartz, E., Girayes, R., Mendelson, A., and Bronstein, A. M. Nice: Noise injection and clamping estimation for neural network quantization. *arXiv preprint arXiv:1810.00162*, 2018.
- Bengio, Y., Léonard, N., and Courville, A. Estimating or propagating gradients through stochastic neurons for conditional computation. *arXiv preprint arXiv:1308.3432*, 2013.
- Cai, Z., He, X., Sun, J., and Vasconcelos, N. Deep learning with low precision by half-wave gaussian quantization. *arXiv preprint arXiv:1702.00953*, 2017.
- Choi, J., Chuang, P. I.-J., Wang, Z., Venkataramani, S., Srinivasan, V., and Gopalakrishnan, K. Bridging the accuracy gap for 2-bit quantized neural networks (qnn). *arXiv preprint arXiv:1807.06964*, 2018a.
- Choi, J., Wang, Z., Venkataramani, S., Chuang, P. I.-J., Srinivasan, V., and Gopalakrishnan, K. Pact: Parameterized clipping activation for quantized neural networks. *arXiv preprint arXiv:1805.06085*, 2018b.
- Choi, Y., El-Khamy, M., and Lee, J. Learning low precision deep neural networks through regularization. *arXiv preprint arXiv:1809.00095*, 2018c.
- Esser, S. K., Merolla, P. A., Arthur, J. V., Cassidy, A. S., Appuswamy, R., Andreopoulos, A., Berg, D. J., McKinstry, J. L., Melano, T., Barch, D. R., di Nolfo, C., Datta, P., Amir, A., Taba, B., Flickner, M. D., and Modha, D. S. Convolutional networks for fast, energy-efficient neuromorphic computing. *Proceedings of the National Academy of Sciences*, 113(41):11441–11446, 2016. ISSN 0027-8424. doi: 10.1073/pnas.1604850113. URL <http://www.pnas.org/content/113/41/11441>.
- He, K., Zhang, X., Ren, S., and Sun, J. Deep residual learning for image recognition. In *Proceedings of the IEEE conference on computer vision and pattern recognition*, pp. 770–778, 2016.
- Hinton, G., Deng, L., Yu, D., Dahl, G. E., Mohamed, A.-r., Jaitly, N., Senior, A., Vanhoucke, V., Nguyen, P., Sainath, T. N., et al. Deep neural networks for acoustic modeling in speech recognition: The shared views of four research groups. *IEEE Signal processing magazine*, 29(6):82–97, 2012.
- Hubara, I., Courbariaux, M., Soudry, D., El-Yaniv, R., and Bengio, Y. Binarized neural networks. In *Advances in neural information processing systems*, pp. 4107–4115, 2016.
- Jouppi, N. P., Young, C., Patil, N., Patterson, D., Agrawal, G., Bajwa, R., Bates, S., Bhatia, S., Boden, N., Borchers, A., et al. In-datacenter performance analysis of a tensor processing unit. In *Computer Architecture (ISCA), 2017 ACM/IEEE 44th Annual International Symposium on*, pp. 1–12. IEEE, 2017.
- Jung, S., Son, C., Lee, S., Son, J., Kwak, Y., Han, J.-J., and Choi, C. Joint training of low-precision neural network with quantization interval parameters. *arXiv preprint arXiv:1808.05779*, 2018.
- Krizhevsky, A., Sutskever, I., and Hinton, G. E. Imagenet classification with deep convolutional neural networks. In *Advances in neural information processing systems*, pp. 1097–1105, 2012.
- Li, F. and Liu, B. Ternary weight networks.(2016). *arXiv preprint arXiv:1605.04711*, 2016.
- Loshchilov, I. and Hutter, F. SGDR: stochastic gradient descent with restarts. *CoRR*, abs/1608.03983, 2016. URL <http://arxiv.org/abs/1608.03983>.
- McKinstry, J. L., Esser, S. K., Appuswamy, R., Bablani, D., Arthur, J. V., Yildiz, I. B., and Modha, D. S. Discovering low-precision networks close to full-precision networks for efficient embedded inference. *arXiv preprint arXiv:1809.04191*, 2018.
- Mishra, A. K. and Marr, D. Apprentice: Using knowledge distillation techniques to improve low-precision network accuracy. *CoRR*, abs/1711.05852, 2017. URL <http://arxiv.org/abs/1711.05852>.
- Polino, A., Pascanu, R., and Alistarh, D. Model compression via distillation and quantization. *arXiv preprint arXiv:1802.05668*, 2018.
- Qiu, J., Wang, J., Yao, S., Guo, K., Li, B., Zhou, E., Yu, J., Tang, T., Xu, N., Song, S., et al. Going deeper with embedded fpga platform for convolutional neural network. In *Proceedings of the 2016 ACM/SIGDA International Symposium on Field-Programmable Gate Arrays*, pp. 26–35. ACM, 2016.
- Rastegari, M., Ordonez, V., Redmon, J., and Farhadi, A. Xnor-net: Imagenet classification using binary convolutional neural networks. In *European Conference on Computer Vision*, pp. 525–542. Springer, 2016.
- Russakovsky, O., Deng, J., Su, H., Krause, J., Satheesh, S., Ma, S., Huang, Z., Karpathy, A., Khosla, A., Bernstein,

M., et al. Imagenet large scale visual recognition challenge. *International Journal of Computer Vision*, 115(3): 211–252, 2015.

Sung, W., Shin, S., and Hwang, K. Resiliency of deep neural networks under quantization. *arXiv preprint arXiv:1511.06488*, 2015.

Xu, H., Gao, Y., Yu, F., and Darrell, T. End-to-end learning of driving models from large-scale video datasets. *arXiv preprint*, 2017.

Zhang, D., Yang, J., Ye, D., and Hua, G. Lq-nets: Learned quantization for highly accurate and compact deep neural networks. *arXiv preprint arXiv:1807.10029*, 2018.

Zhou, S., Wu, Y., Ni, Z., Zhou, X., Wen, H., and Zou, Y. Dorefa-net: Training low bitwidth convolutional neural networks with low bitwidth gradients. *arXiv preprint arXiv:1606.06160*, 2016.

Zhu, C., Han, S., Mao, H., and Dally, W. J. Trained ternary quantization. *CoRR*, abs/1612.01064, 2016. URL <http://arxiv.org/abs/1612.01064>.